U.S. Department of the Interior
U.S. Geological Survey

Scientific Investigations Map 3261
Sheet 8 of 10
Pamphlet accompanies map

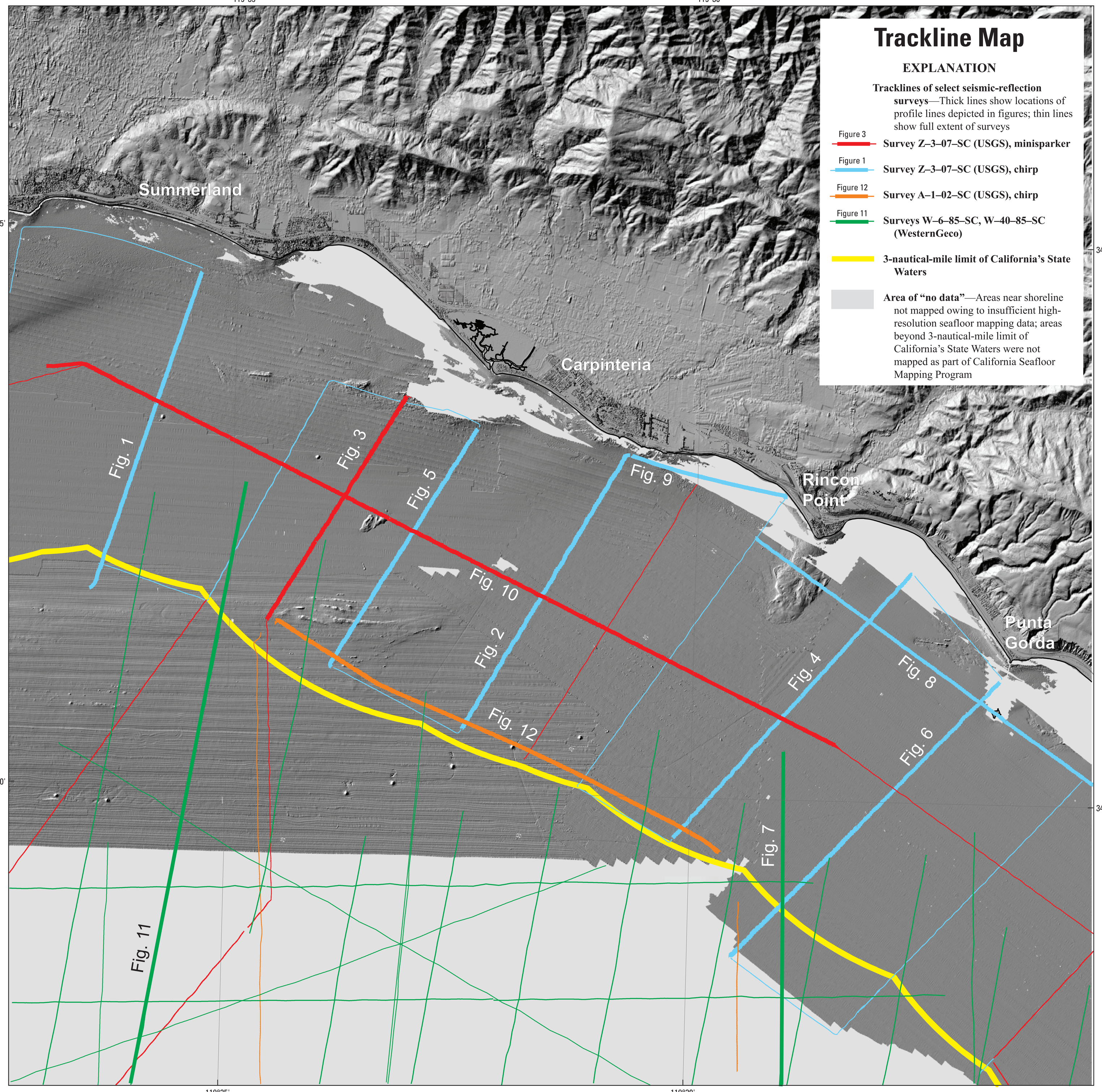

Onshore elevation data from NOAA Coastal Services Center (data collected by EarthData International in 2002-2003) and from U.S. Army Corps of Engineers (data collected by Fugro Pelagos in 2009). Offshore shaded-relief bathymetry from map on sheet 2, this report. California's State Waters limit from NOAA Office of Coast Survey
Universal Transverse Mercator projection, Zone 11N
NOT INTENDED FOR NAVIGATIONAL USE

SCALE 1:50 000
ONE MILE = 0.869 NAUTICAL MILES

APPROXIMATE MEAN DECLINATION, 2013

MAP LOCATION

GIS database and digital cartography by Eleyne L. Phillips and Florence L. Wong
Edited by Taryn A. Lindquist
Manuscript approved for publication June 13, 2013

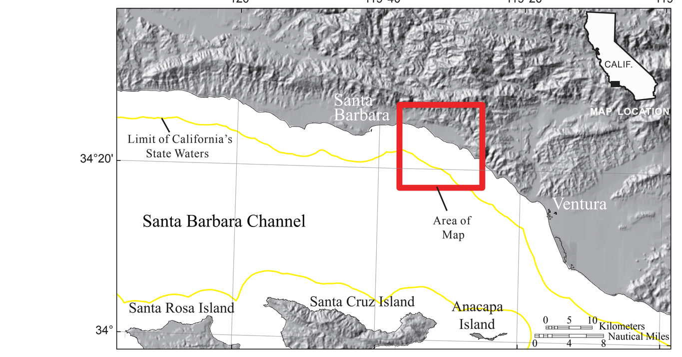

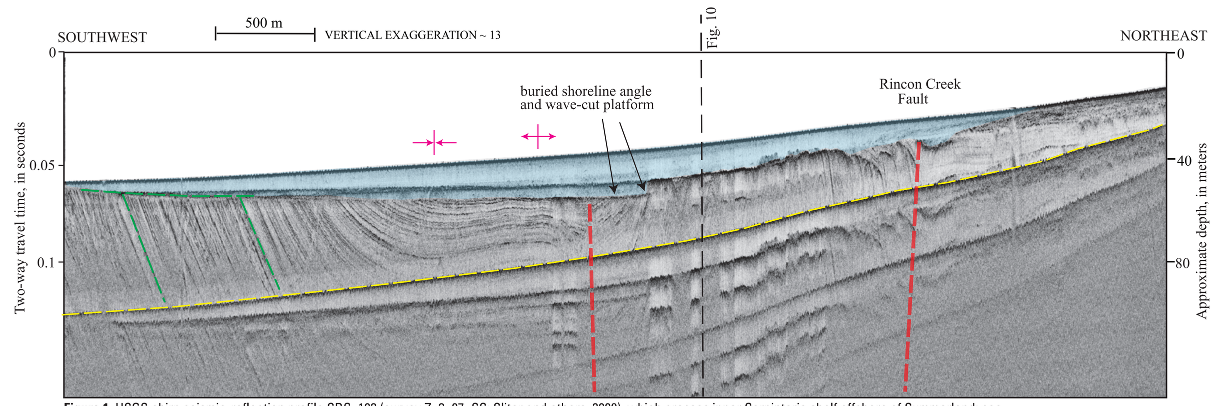

Figure 1. USGS chirp seismic-reflection profile SBC–103 (survey Z–3–07–SC; Sliter and others, 2008), which crosses inner Carpinteria shelf offshore of Summerland; see trackline map for location. Dashed red lines show inferred faults, including Rincon Creek Fault, mapped onshore by Minor and others (2009). Magenta symbols above seafloor show fold axes (diverging arrows, anticline; converging arrows, syncline). Blue shading shows inferred uppermost Pleistocene and Holocene nearshore and shelf deposits, which have maximum thickness of about 17 m on this transect. Buried shoreline indicates location and approximate depth (about 53 m) of sea cliff and wave-cut platform associated with lower sea levels. Dashed green lines highlight part of angular unconformity that separates upper unit from underlying tilted Miocene and younger strata. Dashed yellow line is seafloor multiple (echo of seafloor reflector).

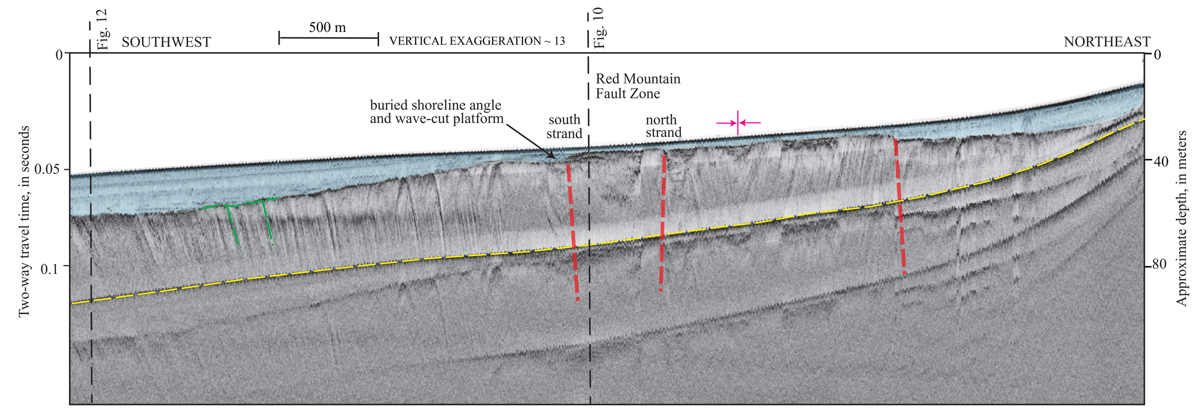

Figure 2. USGS chirp seismic-reflection profile SBC–92 (survey Z–3–07–SC; Sliter and others, 2008), which crosses inner Carpinteria shelf offshore of Carpinteria; see trackline map for location. Dashed red lines show inferred faults, including north and south strands of Red Mountain Fault Zone. Magenta symbol above seafloor shows syncline axis. Blue shading shows inferred uppermost Pleistocene and Holocene nearshore and shelf deposits, which have maximum thickness of about 15 m on this transect but thin over crest of rocky uplift in middle of profile. Upper unit is underlain by prominent angular unconformity; dashed green lines locally highlight discordance. Buried shoreline angle and wave-cut platform is in center of profile, at depth of about 38 m. Dashed yellow line is seafloor multiple (echo of seafloor reflector).

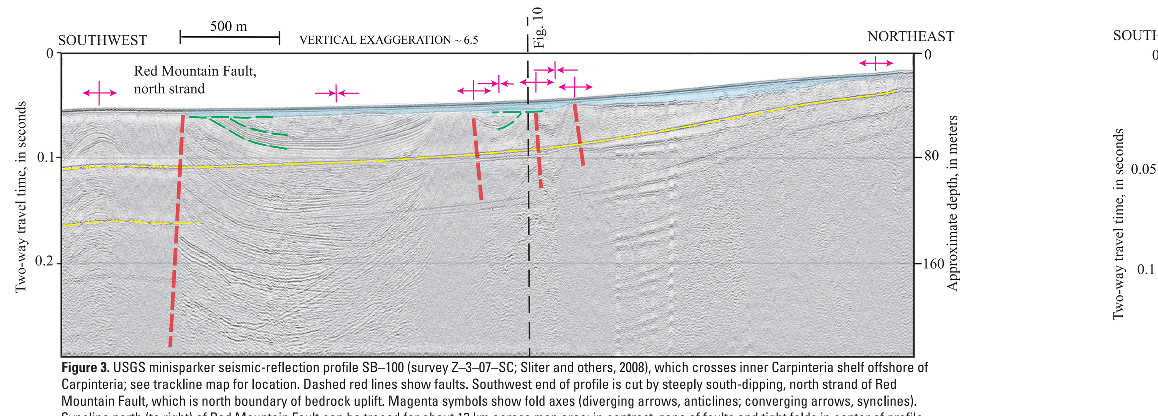

Figure 3. USGS minisparker seismic-reflection profile SB–100 (survey Z–3–07–SC; Sliter and others, 2008), which crosses inner Carpinteria shelf offshore of Carpinteria; see trackline map for location. Dashed red lines show faults. Southwest end of profile is cut by steeply south-dipping, north strand of Red Mountain Fault, which is north boundary of bedrock uplift. Magenta symbols show fold axes (diverging arrows, anticlines; converging arrows, synclines). Syncline north (to right) of Red Mountain Fault can be traced for about 13 km across map area; in contrast, zone of faults and tight folds in center of profile appears to be discontinuous. Blue shading shows inferred uppermost Pleistocene and Holocene nearshore and shelf deposits, which have maximum thickness of about 9 m on this transect. Upper unit is underlain by prominent angular unconformity; dashed green lines partly highlight discordance. Dashed yellow line is seafloor multiple (echo of seafloor reflector).

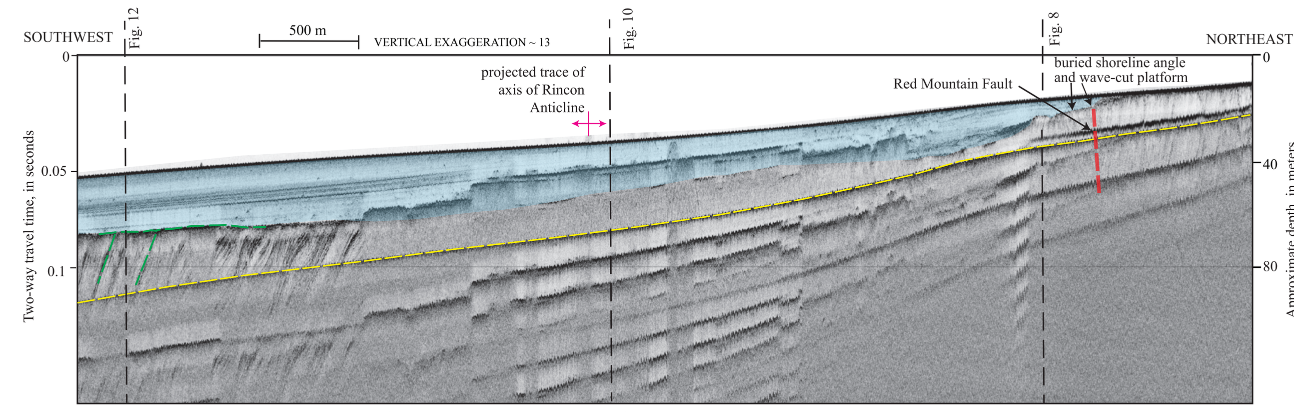

Figure 4. USGS chirp seismic-reflection profile SBC–88 (survey Z–3–07–SC; Sliter and others, 2008), which crosses inner Carpinteria shelf offshore of Rincon Point; see trackline map for location. Dashed red line shows projected trace of Red Mountain Fault. Magenta symbol above seafloor shows anticline axis. Blue shading shows inferred uppermost Pleistocene and Holocene nearshore and shelf deposits, which have maximum thickness of about 24 m on this transect but pinch out at shallow, northeast end of profile. Upper unit is underlain by prominent angular unconformity; dashed green lines partly highlight discordance. Reflections in significant parts of profile are obscured by gas, which may be using faults as conduits for upward migration; this is most obvious near projected axis of Rincon Anticline, along which numerous petroleum fields are located (Barnum, 1998). Dashed yellow line is seafloor multiple (echo of seafloor reflector).

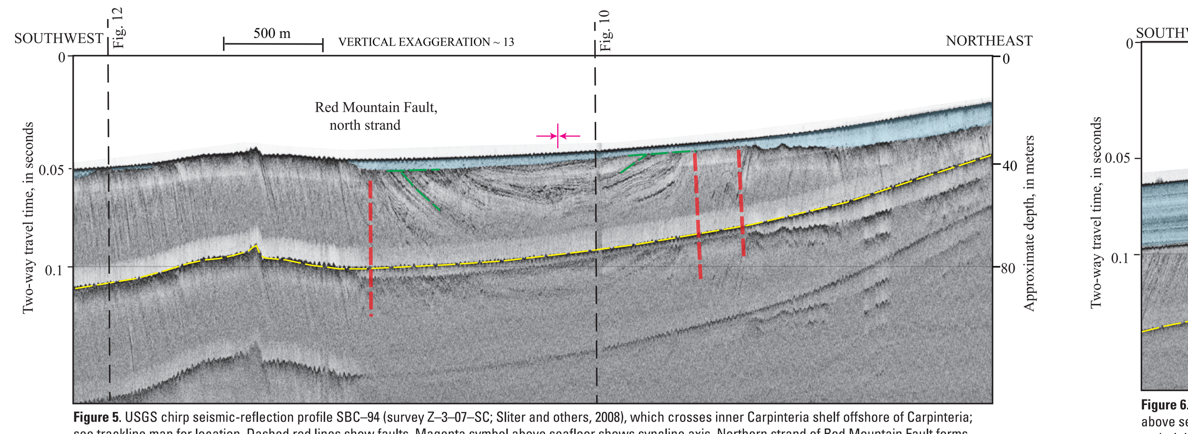

Figure 5. USGS chirp seismic-reflection profile SBC–94 (survey Z–3–07–SC; Sliter and others, 2008), which crosses inner Carpinteria shelf offshore of Carpinteria; see trackline map for location. Dashed red lines show faults. Magenta symbol above seafloor shows syncline axis. Northern strand of Red Mountain Fault forms north boundary of bedrock uplift; faults farther north in center of profile correlate with zone of faulting and tight folding shown in center of figure 2. Blue shading shows inferred uppermost Pleistocene and Holocene nearshore and shelf deposits, which have maximum thickness of about 8 m on this transect but are absent over offshore rocky uplift that is probably underlain by the Pliocene and Pleistocene Pico Formation (see Redin and others, 1998). Upper unit is underlain by prominent angular unconformity; dashed green lines partly highlight discordance. Dashed yellow line is seafloor multiple (echo of seafloor reflector).

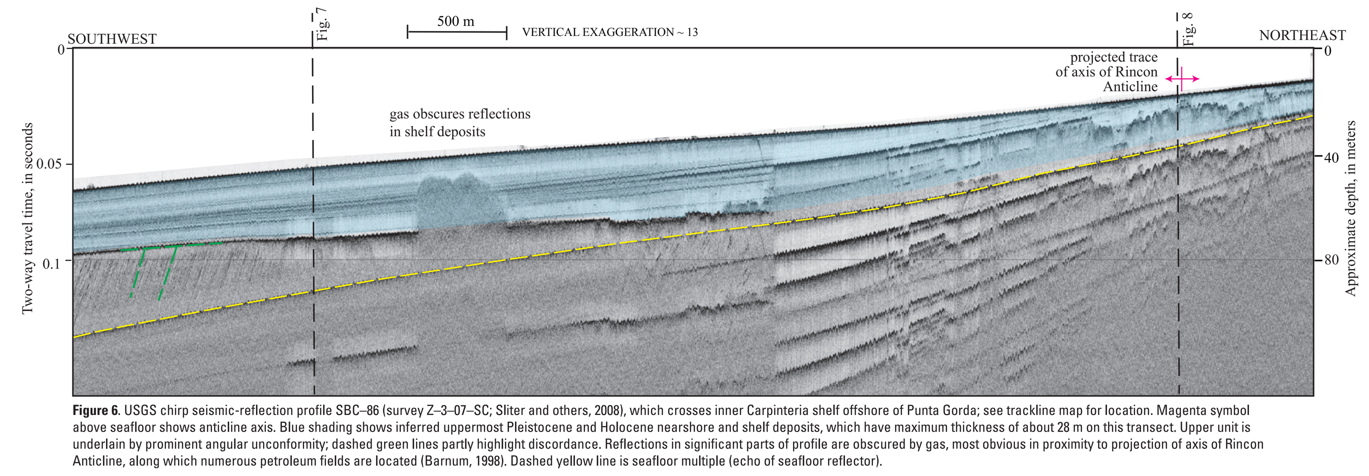

Figure 6. USGS chirp seismic-reflection profile SBC–86 (survey Z–3–07–SC; Sliter and others, 2008), which crosses inner Carpinteria shelf offshore of Punta Gorda; see trackline map for location. Magenta symbol above seafloor shows anticline axis. Blue shading shows inferred uppermost Pleistocene and Holocene nearshore and shelf deposits, which have maximum thickness of about 28 m on this transect. Upper unit is underlain by prominent angular unconformity; dashed green lines partly highlight discordance. Reflections in significant parts of profile are obscured by gas, most obviously in proximity to projection of axis of Rincon Anticline, along which numerous petroleum fields are located (Barnum, 1998). Dashed yellow line is seafloor multiple (echo of seafloor reflector).

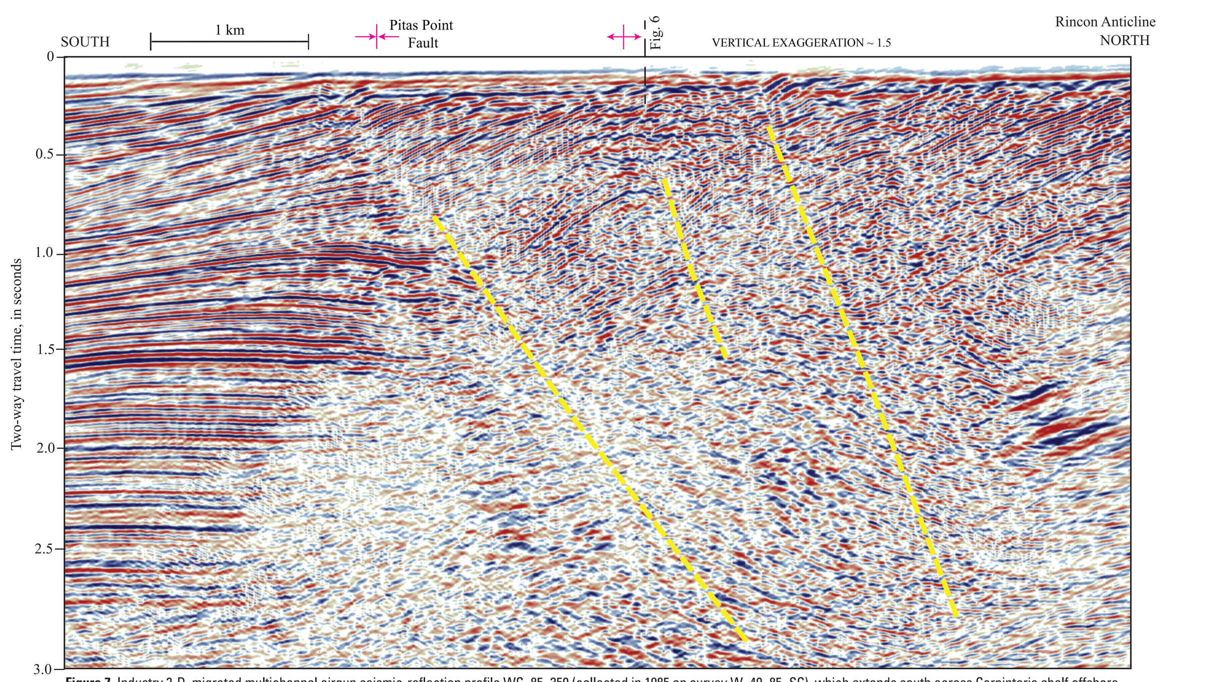

Figure 7. Industry 2-D, migrated multichannel airgun seismic-reflection profile WC–85–350 (collected in 1985 on survey W–40–85–SC), which extends south across Carpinteria shelf offshore of Rincon Point; see trackline map for location. Note that profile has similar horizontal scale to USGS high-resolution seismic-reflection profiles shown in figures 1 through 6, 8 through 10, and 12, but it has much less vertical exaggeration (about 1.5:1). Note also that profile has not been depth converted and so no depth scale is shown, but it probably extends to depths of 4 to 5 km. Dashed yellow lines show inferred faults. Profile reveals predominantly south-dipping strata cut by north-dipping Pitas Point Fault and associated faults. Faults are "blind" at this location and resolution; they appear to fold but not rupture uppermost strata shown in profile. Zone of three north-dipping faults in Pitas Point Fault Zone is similarly represented on cross section in Fisher and others (2009, their fig. 3; modified from Redin and others, 1998), who suggested that faulted stratigraphic section at these depths includes (from oldest to youngest) the Miocene Monterey Formation, the Miocene and Pliocene Sisquoc Formation, the Pliocene Repetto Formation (Galloway, 1997), and the Pliocene and Pleistocene Pico Formation, as well as unnamed Pliocene to Quaternary sedimentary deposits. Magenta symbols above profile show fold axes (diverging arrows, anticline; converging arrows syncline).

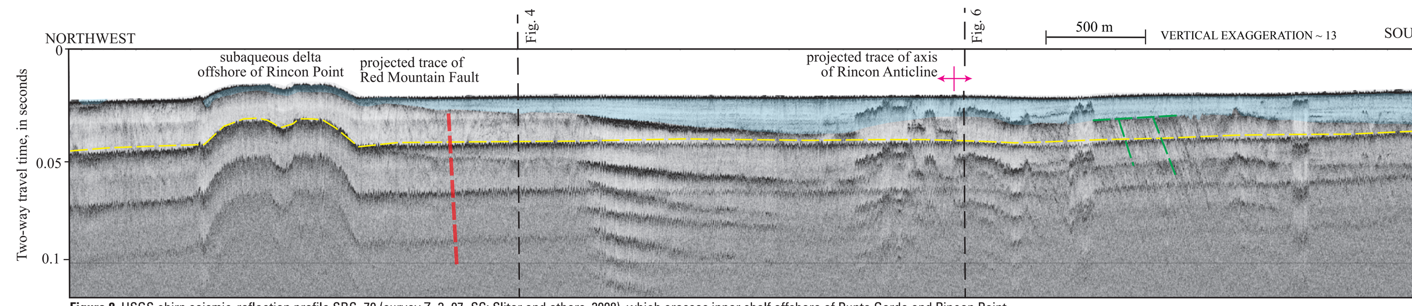

Figure 8. USGS chirp seismic-reflection profile SBC–70 (survey Z–3–07–SC; Sliter and others, 2008), which crosses inner shelf offshore of Punta Gorda and Rincon Point, subparallel to shoreline; see trackline map for location. Dashed red line shows projected trace of Red Mountain Fault. Magenta symbol above seafloor shows anticline axis. Blue shading shows inferred uppermost Pleistocene and Holocene nearshore and shelf deposits, which have maximum thickness of about 14 m on this transect. Upper unit is underlain by prominent angular unconformity; dashed green lines partly highlight discordance. Reflections in much of profile are obscured by gas, most obvious in proximity to axis of productive Rincon Anticline, along which numerous petroleum fields are located (Barnum, 1998). Dashed yellow line is seafloor multiple (echo of seafloor reflector).

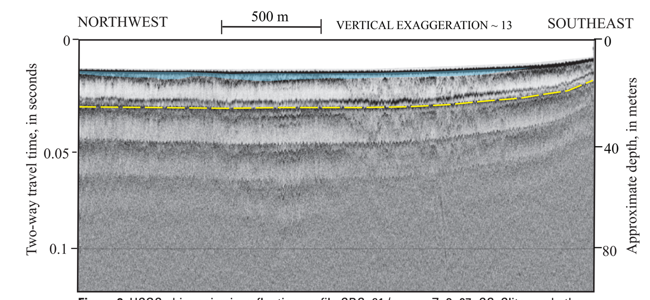

Figure 9. USGS chirp seismic-reflection profile SBC–91 (survey Z–3–07–SC; Sliter and others, 2008), which crosses inner shelf northwest of Rincon Point, subparallel to shoreline; see trackline map for location. Blue shading shows inferred uppermost Pleistocene and Holocene nearshore and shelf deposits, which have maximum thickness of only about 2.5 m on this transect and are absent approaching Rincon Point at southeast end of profile. Dashed yellow line is seafloor multiple (echo of seafloor reflector).

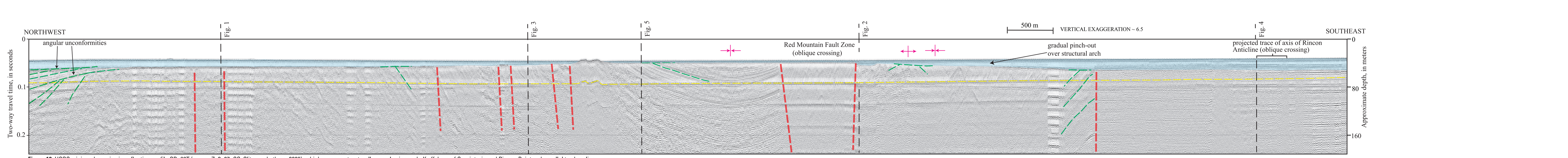

Figure 10. USGS minisparker seismic-reflection profile SB–98T (survey Z–3–07–SC; Sliter and others, 2008), which crosses structurally complex inner shelf offshore of Carpinteria and Rincon Point, subparallel to shoreline; see trackline map for location. Dashed red lines show faults, including oblique crossing of active Red Mountain Fault Zone. Magenta symbols above seafloor show fold axes (diverging arrows, anticlines; converging arrows, synclines). Blue shading shows uppermost Pleistocene and Holocene nearshore and shelf deposits, which unconformably overlie folded Neogene strata; dashed green lines partly show this angular unconformity, as well as older unconfomity within Neogene section. Dashed yellow line is seafloor multiple (echo of seafloor reflector).

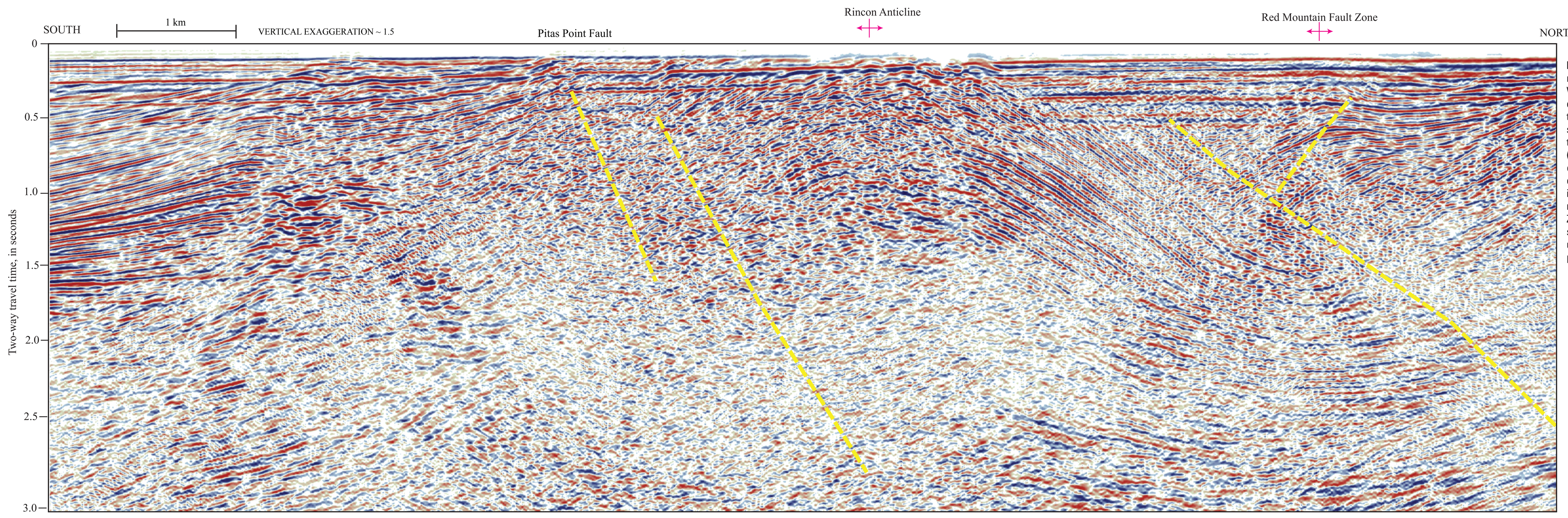

Figure 11. Industry 2-D, migrated multichannel air-gun seismic-reflection profile WC–85–192 (collected in 1985 on survey W–40–85–SC), which extends south across Carpinteria shelf offshore of Summerland; see trackline map for location. Note that profile has similar horizontal scale to USGS high-resolution seismic-reflection profiles shown in figures 1 through 6, 8 through 10, and 12, but it has much less vertical exaggeration (about 1.5:1). Note also that profile has not been depth converted and so no depth scale is shown, but it probably extends to depths of 4 to 5 km. Dashed yellow lines show inferred faults. Profile reveals broadly folded strata cut by north-dipping, blind Pitas Point Fault and Red Mountain Fault Zone (sheet 10), which includes south-dipping back splay (note shallow deformation). Faults appear to fold but not rupture uppermost strata shown in profile. Magenta symbols above profile show anticline axes.

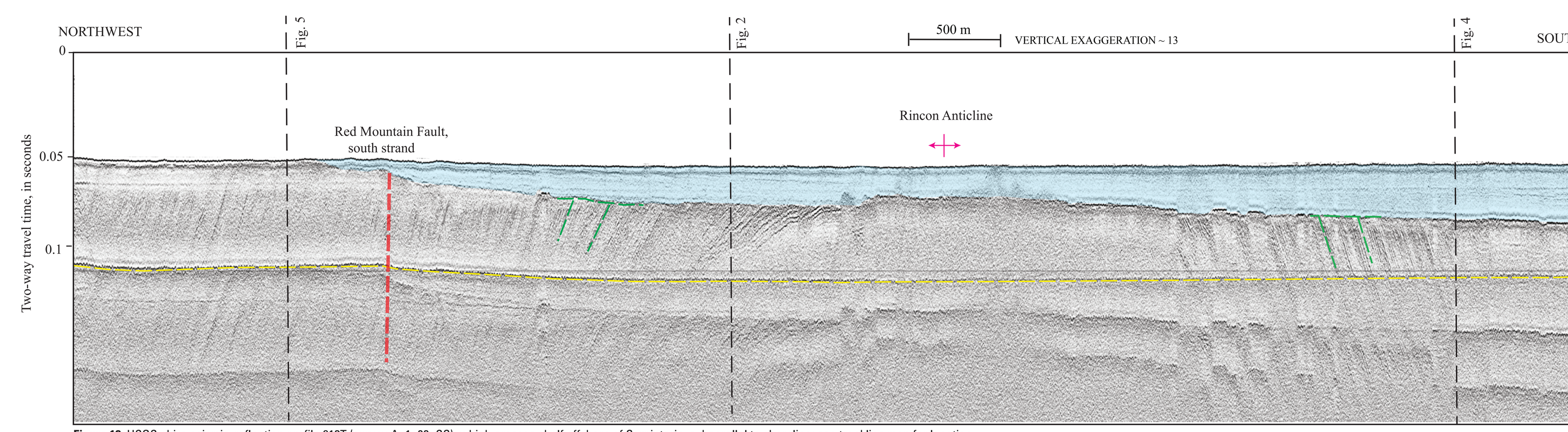

Figure 12. USGS chirp seismic-reflection profile 813T (survey A–1–02–SC), which crosses shelf offshore of Carpinteria, subparallel to shoreline; see trackline map for location. Dashed red line shows inferred fault. Magenta symbol above seafloor shows anticline axis. Blue shading shows inferred uppermost Pleistocene and Holocene nearshore and shelf deposits, which have maximum thickness of about 22 m on this transect but pinch out over bedrock uplift in northwestern part of profile. Upper unit is underlain by prominent angular unconformity; dashed green lines partly highlight discordance. Dashed yellow line is seafloor multiple (echo of seafloor reflector).

DISCUSSION

This map sheet shows seismic-reflection profiles from three different surveys of the Offshore of Carpinteria map area, providing imagery of the subsurface geology. The area is characterized by a broad, relatively shallow (less than 40 m) wave-cut shelf. The shelf is relatively flat (less than 0.5°) but has local relief associated with bedrock uplifts. The seismic-reflection data reveal that the shelf is underlain by variably thick (0 m to about 35 m) upper Pleistocene and Holocene marine, deltaic, and alluvial strata (blue shading in profiles; Dahlen, 1992; Slater and others, 2002; Draut and others, 2009; Sommerfield and others, 2009) deposited in the last about 21,000 years, following the last major sea-level lowstand (see, for example, Fleming and others, 1998). These young sediments unconformably overlie folded Neogene and Quaternary strata that include the Miocene Monterey Formation, the Miocene and Pliocene Sisquoc Formation, and the Pliocene and Pleistocene Pico Formation (Redin and others, 1998).

The presence and continuity of seismic reflections in the upper sediment unit on many profiles is obscured by interstitial gas within the sediments. This effect has been referred to as "gas blanking," "acoustic turbidity," or "acoustic masking" (Fader, 1997). The gas scatters or attenuates the acoustic energy, preventing penetration. Not surprisingly, this effect is especially prevalent along the projected trace of the Rincon Anticline (the offshore extension of the Ventura Avenue Anticline) (figs. 4, 6, 8, 10, 12), a geologic structure that hosts numerous actively producing oil fields (see, for example, Barnum, 1998).

The seismic profiles show significant folding and three important active faults. The north-dipping, east-west-striking Pitas Point Fault, which crosses the southern part of the map area, is interpreted as a blind-thrust or blind-reverse fault beneath the Rincon Anticline (fig. 11; see also, Redin and others, 1998). Deeper industry seismic-reflection profiles (figs. 7, 11) reveal at least two other north-dipping blind-reverse faults in the hanging wall of the Pitas Point Fault. Farther north, the seismic profiles show the east-west-striking Red Mountain Fault as a single strand to the east that bifurcates westward into a south-dipping north strand and a north-dipping south strand (see sheets 9, 10). This fault offsets late Quaternary terraces on land (Trecker and others, 1998) and significantly influences regional sediment thicknesses in the offshore (see sheet 9). Still farther north, the east-west-striking Rincon Creek Fault has been interpreted as a south-dipping, reverse-fault splay off the Red Mountain Fault (Redin and others, 1998). The Rincon Fault, which clearly warps uppermost Pleistocene to Holocene strata, appears to be displaced by a north-south-striking tear fault in the western part of the map area.

Most profiles displayed on this map sheet (figs. 1, 2, 3, 4, 5, 6, 8, 9, 10) were collected in 2007 on U.S. Geological Survey (USGS) cruise Z–3–07–SC (Sliter and others, 2008). Single-channel seismic-reflection data were acquired using two different sources, the EdgeTech 512 chirp (figs. 1, 2, 4, 5, 6, 8, 9) and the SIG 2Mille minisparker (figs. 3, 10). The EdgeTech 512 chirp subbottom-profiling system consists of a source transducer and an array of receiving hydrophones housed in a 500-lb fish towed at a depth of several meters below the sea surface. The swept-frequency chirp source signal was 500 to 4,500 Hz and 50 ms in length, and it was recorded by hydrophones located on the bottom of the fish. The SIG minisparker system used a 500-J high-voltage electrical discharge fired 1 to 4 times per second, which, at normal survey speed of 4 to 4.5 nautical miles per hour, gives a data trace every 0.5 to 2.0 meters. The data were digitally recorded in standard SEG-Y 32-bit floating-point format using PC-based Triton Subbottom Logger (SBL) software that merges seismic-reflection data with differential GPS-navigation data. After the survey, a short-window (20 ms) automatic gain control algorithm was applied to both the chirp and minisparker data, and a 160- to 1,200-Hz bandpass filter was applied to the minisparker data. The vertical scale on the high-resolution seismic-reflection profiles (figs. 1, 2, 3, 4, 5, 6, 8, 9, 10) is shown as two-way travel time in seconds, as well as in meters on the basis of an inferred velocity of 1,600 m/sec for near-surface sediments.

Figures 7 and 11 show deep-penetration, migrated, multichannel seismic-reflection profiles collected in 1985 by WesternGeco on cruise W–40–85–SC. These profiles and other similar data were collected in many areas offshore of California in the 1970s and 1980s when the area was considered a frontier for oil and gas exploration. Much of these data have been publicly released and are now archived at the USGS National Archive of Marine Seismic Surveys (U.S. Geological Survey, 2009). These data were acquired with a large-volume air-gun source that has a frequency range of 3 to 40 Hz and recorded with a multichannel hydrophone streamer about 2 km long; shot spacing was about 30 m. These data can resolve geologic features that are 20 to 30 m thick (large-scale features), down to subbottom depths of about 4 km.

REFERENCES CITED

Barnum, H.P., 1998, Redevelopment of the western portion of the Rincon offshore oil field, Ventura, California, *in* Kunitomi, D.S., Hopps, T.E., and Galloway, J.M., eds., Structure and petroleum geology, Santa Barbara Channel, California: American Association of Petroleum Geologists, Pacific Section, and Coast Geological Society, Miscellaneous Publication 46, p. 201–215.

Dahlen, M.Z., 1992, Sequence stratigraphy, depositional history, and middle to late Quaternary sea levels of the Ventura shelf, California: Quaternary Research, v. 38, p. 234–245.

Draut, A.E., Hart, P.E., Lorenson, T.D., Ryan, H.F., Wong, F.L., Sliter, R.W., and Conrad, J.E., 2009, Late Pleistocene to Holocene sedimentation and hydrocarbon seeps on the continental shelf of a steep, tectonically active margin, southern California, USA: Marine Geophysical Research, v. 30, p. 193–206, doi:10.1007/s11001-009-9076-y.

Fader, G.B.J., 1997, Effects of shallow gas on seismic-reflection profiles, *in* Davies, T.A., Bell, T., Cooper, A.K., Josenhaus, H., Polyak, L., Solheim, A., Stoker, M.S., and Stravers, J.A., eds., Glaciated continental margins—An atlas of acoustic images: London, Chapman & Hall, p. 29–30.

Fisher, M.A., Sorlien, C.C., and Sliter, R.W., 2009, Potential earthquake faults offshore southern California from the eastern Santa Barbara channel to Dana Point, *in* Lee, H.J., and Normark, W.R., eds., Earth science in the urban ocean—The Southern California Continental Borderland: Geological Society of America Special Paper 454, p. 271–290.

Fleming, K., Johnston, P., Zwartz, D., Yokoyama, Y., Lambeck, K., and Chappell, J., 1998, Refining the eustatic sea-level curve since the Last Glacial Maximum using far- and intermediate-field sites: Earth and Planetary Science Letters, v. 163, p. 327–342, doi:10.1016/S0012-821X(98)00198-8.

Galloway, J.M., 1997, Santa Barbara-Ventura basin province, *in* Dunkel, C.A., and Piper, K.A. eds., 1995 National assessment of United States oil and gas resources assessment of the Pacific outer continental shelf region: Minerals Management Service, Pacific OCS Region, Office of Resource Evaluation, OCS Report MMS 92–0019, p. 96–115.

Minor, S.A., Kellogg, K.S., Stanley, R.G., Gurrola, L.D., Keller, E.A., and Brandt, T.R., 2009, Geologic map of the Santa Barbara coastal plain area, Santa Barbara County, California: U.S. Geological Survey Scientific Investigations Map 3001, scale 1:25,000, 1 sheet, pamphlet 38 p., available at http://pubs.usgs.gov/sim/3001/.

Redin, T., Forman, J., and Kamerling, M.J., 1998, Regional structure section across the eastern Santa Barbara channel, from eastern Santa Cruz Island to the Carpinteria area, Santa Ynez Mountains, *in* Kunitomi, D.S., Hopps, T.E., and Galloway, J.M., eds., Structure and petroleum geology, Santa Barbara Channel, California: American Association of Petroleum Geologists, Pacific Section, and Coast Geological Society, Miscellaneous Publication 46, p. 195–200, 1 sheet.

Slater, R.A., Gorsline, D.S., Kolpack, R.L., and Shiller, G.I., 2002, Post-glacial sediments of the California shelf from Cape San Martin to the US-Mexico border: Quaternary International, v. 92, p. 45–61.

Sliter, R.W., Triezenberg, P.J., Hart, P.E., Draut, A.E., Normark, W.R., and Conrad, J.E., 2008, High-resolution chirp and mini-sparker seismic-reflection data from the southern California continental shelf—Gaviota to Mugu Canyon: U.S. Geological Survey Open-File Report 2008–1246, accessed April 5, 2011, at http://pubs.usgs.gov/of/2008/1246/.

Sommerfield, C.R., Lee, H.J., and Normark, W.R., 2009, Postglacial sedimentary record of the southern California continental shelf and slope, Point Conception to Dana Point, *in* Lee, H.J., and Normark, W.R., eds., Earth science in the urban ocean—The Southern California Continental Borderland: Geological Society of America Special Paper 454, p. 89–116.

Trecker, M.A., Gurrola, L.D., and Keller, E.A., 1998, Oxygen-isotope correlation of marine terraces and uplift of the Mesa Hills, Santa Barbara, California, USA, *in* Stewart, I.S., and Vita-Finzi, C., eds., Coastal tectonics: Geological Society of London Special Publications, v. 146, p. 57–69.

U.S. Geological Survey, 2009, National Archive of Marine Seismic Surveys: U.S. Geological Survey database, accessed April 5, 2011, at http://walrus.wr.usgs.gov/NAMSS/.

Seismic-Reflection Profiles, Offshore of Carpinteria Map Area, California

By
Samuel Y. Johnson, Ray W. Sliter, Amy E. Draut, Andrew C. Ritchie, and Eleyne L. Phillips
2013

For sale by U.S. Geological Survey, Information Services, Box 25286, Federal Center, Denver, CO 80225, 1-888-ASK-USGS
Digital files available at http://pubs.usgs.gov/sim/3261/